Oki, K., W. P. Walawender, and L. T. Fan, "The Measurement of Local Velocity of Solid Particles," *Powder Tech.*, **18**, 171 (1977).
Oki, K., M. Ishida, and T. Shirai, "The Behavior of Jets and Particles near the Gas Distributor Grid in a Three-Dimensional Fluidized Bed," *Proc. Int. Conf. Fluidization*, 421, Henniker, New Hampshire, (1980).
Tennekes, H., and J. L. Lumley, *A First Course in Turbulence*, 224, MIT Press, Cambridge, MA (1972).
Velzen, D. V., et al., "Motion of Solids in Spouted Beds," *Can. J. Chem. Eng.*, **52**, 156 (1974).
Verloop, J., and P. M. Heertjes, "Periodic Pressure Fluctuations in Fluidized Bed," *Chem. Eng. Sci.*, **29**, 1035 (1974).
Werther, J., and O. Molerus, "The Local Structure of Gas Fluidized Beds. II: The Spatial Distribution of Bubbles," *Int. J. Multiphase Flow*, **1**, 123 (1973).
Whitehead, A. B., G. Gartside, and D. C. Dent, "Fluidization Studies in Large Gas-Solid Systems. III: The Effect of Bed Depth and Fluidizing Velocity on Solids Circulation Patterns," *Powder Technol.*, **14**, 61 (1976).

Manuscript received Feb. 16, 1983; revision received Oct. 31, 1983, and accepted Nov. 11.

Transport Processes in Narrow (Capillary) Channels

Rates of mass and momentum transport in narrow flow channels (gaps 0.2–0.5 mm) have been determined over a wide range of flow velocities, 220–7,700 cm/sec (Re 1,300 to 22,000). Existing correlations that apply to smooth channels of much larger hydraulic diameter were found to be valid for the narrow channels as well. However, in the turbulent regime the condition of hydraulic smoothness could be satisfied only when the walls were optically smooth. Transport rates to rough walls were also measured. The ratio of the mass transport to the momentum transport in the form of $j_D/(f/2)$—a measure of the improved mass transfer compared to the increased pressure drop—is given for the smooth and rough-wall cells over the Re range studied.

R. E. ACOSTA,
R. H. MULLER,
and C. W. TOBIAS

Lawrence Berkeley Laboratory
University of California, Berkeley
Berkeley, CA 94720

SCOPE

The use of very thin channels for the purpose of heat or mass transfer is becoming widespread for a number of applications, including nuclear reactors, electrochemical machining, and electro-organic syntheses. Empirical correlations available to calculate rates of momentum and mass transport in the turbulent regime have been obtained using flow channels with an equivalent diameter of 2 cm or more. In the present work the applicability of these correlations to mass transfer in very thin channels (fractions of a millimeter) was tested. Because of the very large pressure drops involved in processes using very thin channels, the expenditure in pumping power becomes an important economic consideration. Accordingly, the conditions under which maximum mass transfer (or heat dissipation) may be achieved with a minimum pressure drop were also studied. Rates of mass transfer were determined using an electrochemical technique: measurement of limiting currents. The rates of momentum transport were determined by measuring the pressure drop in the same channels where the mass transport rates were measured. For the very small hydraulic diameters employed in this work it was found that the condition of hydraulic smoothness could be satisfied only when the walls of the channel were optically smooth. Because in practical situations the latter condition is seldom found, four degrees of roughness were employed in addition to smooth walls.

CONCLUSIONS AND SIGNIFICANCE

Coefficients for mass and momentum transport in rectangular cross-sectional channels with equivalent diameters of 0.096 and 0.038 cm have been successfully determined in the Reynolds number range of 1,300 to 22,000. At the largest Reynolds numbers employed, an equivalent mass transfer boundary-layer thickness of 2.3×10^{-5} cm was obtained. Mass transfer boundary layers as thin as this do not appear to have been previously reported for channel flows.

The coefficients of mass and momentum transport in smooth rectangular channels with wall separations in the range of fractions of a millimeter can successfully be correlated by the equations that apply to smooth channels of much larger equivalent diameter. However, for thin channels to be considered hydraulically smooth at $Re \geq 2{,}500$, the walls must be polished to optical smoothness. Since this condition is rarely encountered in practical applications, care must be exercised in extrapolating results obtained with large equivalent diameter channels.

Under conditions where the Reynolds number falls in the laminar regime, only very gross surface roughness has an effect on the value of the transport coefficients. For smooth surfaces the mass transfer rate is given by the extension to the Graetz-Leveque solution:

$$Sh_{ave} = 1.85\,(ReScD_h/x)^{1/3}$$

Correspondence concerning this paper should be addressed to R. E. Acosta. Present address: IBM T. J. Watson Research Center, P.O. Box 218, Yorktown Heights, NY 10598.

In the turbulent regime, $Re \geq 10{,}000$, for smooth surfaces (see above), the value of the mass transfer coefficient is satisfactorily predicted by the Chilton-Colburn correlation:

$$Sh_{ave} = (f/2)ReSc^{1/3}$$

where f is given by the Blasius equation $f = 0.079\ Re^{-1/4}$.

When the surfaces are rough, the ratio of the mass transfer coefficient to the friction factor depends strongly on the type and degree of roughness of the surface. For the two largest roughness values employed in this study, this ratio had well-defined maxima in the range $2{,}700 \leq Re \geq 10{,}000$. The gain in improved mass transfer relative to the increase in pressure drop, $j_D/(f/2)$, is of great importance in assessing the effectiveness of narrow gap cells, since their operation is limited by the requirement for very large pumping power. Lacking a good theory to predict the hydrodynamics on rough surfaces, the dependence of $j_D/(f/2)$ ratio on Re for industrial electrolytic cells with very small D_h will have to be determined experimentally.

The present study does not attempt to provide a detailed analysis of entrance phenomena. The approximate results obtained indicate that in the turbulent regime the mass transfer entrance length declined from 10 D_h at $Re = 5 \times 10^3$ to 2.5 D_h at $Re = 2 \times 10^4$.

The conclusion that correlations developed for large D_h channels are applicable to thin channels—provided that careful attention is given to the effect of surface roughness—should be applicable to the problem of heat transfer in very narrow slits (e.g., in nuclear reactors). It is not claimed here that an exact analogy exists between the two transfer processes. However, departure from the behavior observed in systems involving large D_h would more likely occur in mass transfer experiments, where the boundary layer is thin (i.e., large Schmidt number). Since significant discrepancies were not observed in the present study, one can reasonably expect that heat transfer correlations obtained for large D_h (and small Pr number) would also be applicable to heat transfer in very thin channels.

Future work using very small equivalent diameters should extend the present results to Reynolds numbers larger than 22,000 to attain fully developed turbulence. The experimental difficulties involved in this type of endeavor will be significant because of the large pressure drops associated with operation at high Reynolds numbers.

INTRODUCTION

In recent years the use of thin channels for the purpose of heat or mass transfer has been required in a variety of applications. In nuclear reactors circulation channels for the coolant with a width of 1 cm or less are not uncommon. Use of very thin channels (50 μm) to fulfill heat transfer requirements of dense semiconductor (VLSI) chips is being explored (Tuckerman and Pease, 1981). In the electrochemical industry (e.g., metal refining, electrochemical machining [ECM]), it is necessary to use large current densities to increase the throughput of a given installation. Since the conductivity of aqueous electrolytes is at best of the order of 1.0 $(\Omega \cdot cm)^{-1}$ a current density of 100 A cm^{-2}, commonly used in ECM, involves a rate of production of heat of 10,000 $W \cdot cm^{-3}$ of electrolyte contained between the electrodes. In order to keep the energy losses low, and the heat evolved within tractable limits, these processes have to be conducted using interelectrode separations of fractions of a millimeter; to dissipate the heat, the electrolyte has to flow through the channel at very high flow rates. In the field of electro-organic synthesis the need to maintain very small interelectrode separations to prevent large potential drops, and to ensure thin mass transfer boundary layers, also calls for the use of very thin reactors.

Lack of quantitative understanding of transport processes outside the laminar regime requires reliance upon empirical correlations (obtained using flow channels with an equivalent diameter of 2 cm or more; e.g., Chilton-Colburn, 1934, and Lin et al., 1953) to calculate rates of heat, mass, and momentum transport under turbulent conditions. It was of interest to test the applicability of these correlations to mass transfer in thin channels, since the validity of their extrapolation to flow that occurs in channels involving 2 orders of magnitude smaller equivalent diameters has not been previously ascertained.

Another aspect of great interest is the added cost of pumping when conducting processes using very thin channels. Since the pressure drop for a given Reynolds number is proportional to D_h^{-3}, the expenditure of pumping power for processes using very thin channels becomes an important economic consideration.

The present work involves measurements of the rates of mass and momentum transfer in channels with equivalent diameters of 0.096 and 0.038 cm (0.05 and 0.019 cm gap, respectively), using electrolyte flow rates in the Reynolds number range of 1,300 to 22,000, corresponding to linear velocities of 200 to 7,700 cm/s.

In practical applications electrodes are seldom hydraulically smooth. For the very small equivalent diameters employed in this work it was found that the condition of hydraulic smoothness could be satisfied only when the walls were optically smooth. In addition to polished walls, four different degrees of roughness were also employed. Since the literature on the effect of roughness on transport processes is scant, it was of interest to study the effect that various types of roughness have on the mass transfer coefficient, the friction factor, and the ratio of the mass transfer coefficient to the momentum transfer coefficient, $j_D/(f/2)$.

DETERMINATION OF MASS TRANSPORT COEFFICIENTS

Determination of mass transfer coefficients involved the measurement of limiting currents in the cathodic reduction of ferricyanide ion on nickel electrodes.

The Limiting Current Method

Measurement of limiting currents is an experimental technique that has been quite widely employed in mass transfer experiments (see, e.g., Mizushina et al., 1971; Selman and Tobias, 1978). Its relative simplicity and flexibility make the limiting current method a powerful tool in experimental studies of forced and free convection, as well as in pure diffusion.

In this method increasing current is caused to flow across two electrodes, connected by an electrolyte, by increasing the applied cell voltage until a point is reached where the reaction rate is limited by the supply of reactant to the solution/electrode interface. Under these conditions further increase in the applied potential will not result in increased passage of current until a potential is reached that allows a consecutive reaction to occur. If one constructs a plot of current passing though the electrode against applied potential, the above limitation in reaction rate will be manifested by the appearance of a flat section in the curve, the limiting current plateau. At the limiting current the rate of transport of reactant to the interface is smaller than the rate at which it can potentially be consumed by the charge transfer reaction; as a result, at the interface the concentration of this species approaches zero. The flux of reacting species is given by

$$N = i/nF(1 - t) \qquad (1)$$

When the concentration of the reacting species relative to the total

ionic concentration of the electrolyte is small $t \ll 1$, Eq. 1 becomes

$$N = i/nF \tag{2}$$

From the measured current, a mass transfer coefficient, k, defined by

$$N = k(C_b - C_0) \tag{3}$$

may be calculated. Since at the limiting current we may set $C_b = 0$.

$$k = i_{\lim}/nFC_b \tag{4}$$

Sectioned Electrode

To allow determination of the mass transfer coefficients as a function of distance from the electrode leading edge, sectioned electrodes were employed. In these the continuous planar electrode surface is substituted by closely spaced parallel segments, normal to the channel axis, each insulated electrically from the others. By polarizing each electrode to the same potential this array of segments approximates, for mass transport purposes, a continuous electrode. The difference is that the current to each segment, and hence the mass transfer coefficient, can be measured separately and simultaneously.

Since the limiting current measured is obtained over the finite length of an individual section, the values of $i_{\lim}$ provide an average mass transfer coefficient over that individual section. Assignment of this value to any specific point can, of course, represent only an approximation. From this it follows that accurate determination of the variation of the mass transfer coefficient with downstream distance would necessitate the use of very thin electrode segments to approach point (line) electrodes. However, this scheme carries with it disturbances in the development of the mass transfer boundary layer, since transfer is interrupted at the insulator. Furthermore, there are disturbances of the flow created by the slight discontinuities between the electrode and the insulator sections (see below).

Choice of Electrode Reaction

Two main types of reactions are usable in limiting current measurements: a) deposition of the reacting species at the cathode, and b) reduction/oxidation at the cathode/anode of a species in solution to give a soluble species at the interface.

A redox system, rather than a deposition reaction, was chosen for this study because the latter presents the same problem as experiments using soluble walls, i.e., the surface changes as the experiment progresses. This may alter the hydrodynamic characteristics of the flow past the surface. On the other hand, with redox reactions both the reacting and the product species are in solution, making redox systems an almost ideal choice in forced convection studies. In fact, the ferricyanide system has been used extensively for this purpose in the past 25 years (see, e.g., Eisenberg et al., 1954; van Shaw et al., 1963; Hubbard and Lightfoot, 1966; Son and Hanratty, 1967; Mizushina et al., 1971; Dawson and Trass, 1972; Selman and Tobias, 1978).

The electrolyte used was an aqueous solution of potassium ferrocyanide and potassium ferricyanide, with a relatively high concentration of NaOH as a supporting electrolyte (so that $t \ll 1$, for the reacting ion, ferricyanide). The approximate composition of the solution was $K_3Fe(CN)_6$ 0.04 M, $K_4Fe(CN)_6$ 0.20 M, and NaOH 2.0 M. The reactions at the anode (A) and cathode (C) are

$$Fe(CN)_6^{3-} + e^- \underset{A}{\overset{C}{\rightleftharpoons}} Fe(CN)_6^{4-}$$

The concentration and density of the solution were determined from samples taken daily from the tank immediately before and immediately after completion of a series of experiments. The viscosity and the diffusion coefficients were calculated from a polynomial equation given by Boeffard (1966) and from the equation given by Gordon et al. (1966), respectively.

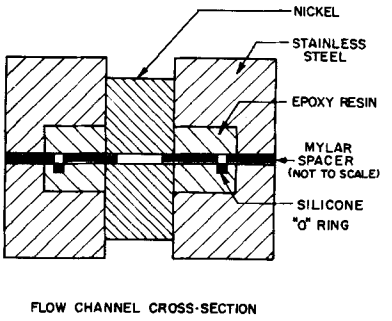

Figure 1. Schematic cross section of the flow cells.

The temperature of the electrolyte was maintained at 22 ± 0.1°C. The tank where the solution was kept was made impervious to light to prevent the slow decomposition of the solution (Eisenberg et al., 1954). For the same reason the solutions were discarded after a few days of use.

Cell Design

The equipment used in this work included two flow channels (Cells I and II) of rectangular cross section in a closed-loop flow circuit. The mass transfer sections (i.e., the electrodes) were formed by facing sections of nickel embedded in the two wide walls of the channel, occupying their entire width (Figures 1 and 2). The minute dimensions of the interelectrode gaps used in this study, together with the very high flow velocities necessary to achieve turbulent flow, require rather exacting specifications in the design of the experimental cells.

The following characteristics were required of the cells: (1) ease in cleaning the electrodes and in refinishing them when necessary; (2) wall strength to withstand a differential pressure along the cell of the order of 20.7×10^6 N/m^2; (3) a precise, uniform, separation between the electrodes; (4) convenient changing of the aspect ratio of the cell; (5) sectioned electrodes to allow measurement of the mass transfer coefficient as a function of distance downstream from the mass transfer leading edge; (6) pressure taps for measurement of the pressure variation in the flow direction; (7) an entrance length before the mass transfer region (the electrodes) sufficient to allow for fully developed flow at that location; and (8) a pressure drop in the cell as small as possible.

These features were obtained using a sandwich type cell formed by bolting together two plates separated by an insulating shim (Figure 3). The two plates were machined of 316 stainless steel to give the necessary wall strength and to make them resistant to attack by spills of the caustic electrolyte employed. The insulating shim was a piece of Mylar sheet.

A slot with the width desired for the channel was cut in the Mylar spacer. When the two plates were bolted together with the Mylar sheet in between them, the edges of the slot in the Mylar formed the side (narrow) walls of the channel and the bounding plates

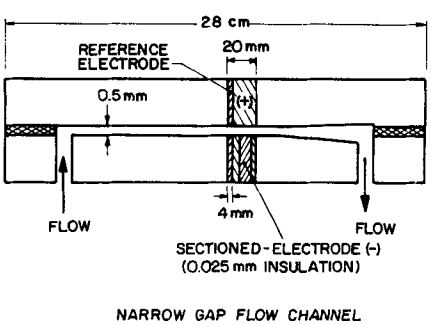

Figure 2. Schematic longitudinal cross section of the flow cells.

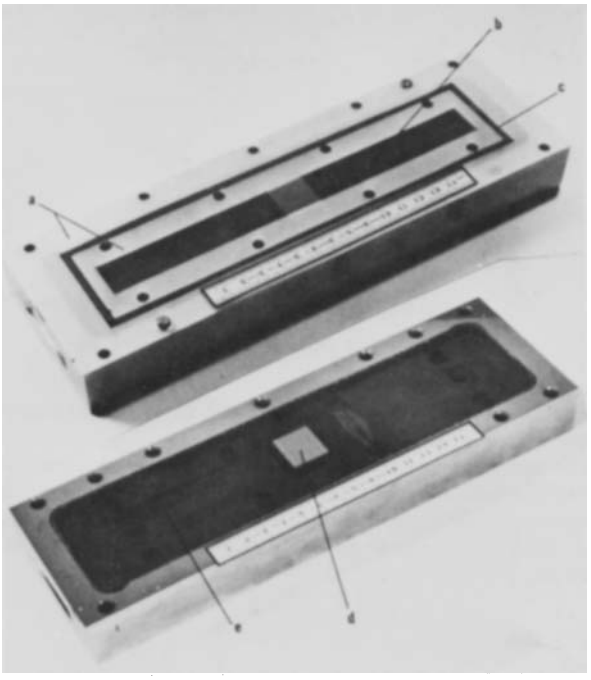

Figure 3. Overall view of Cell I, opened. (a) Mylar spacer. (b) 7° effuser. (c) Silicone "O" ring. (d) Segmented electrode. (e) Capillary pressure tap holes.

formed the wider walls (refer to Figures 1 and 2). Different aspect ratios were in this way easily attainable, by simply exchanging the spacers.

A 0.953 cm deep cavity was milled in the two facing surfaces of the stainless steel plates. This cavity was later filled with an oven-cured epoxy resin. In this manner the channel outside the mass transfer region was nonconducting, preventing stray currents. A rectangular opening milled through the center of the plate housed the sectioned electrode in the finished cell. The distance from the entrance of the channel to the leading edge of the mass transfer section was 7.8 cm in Cell I and 3.73 cm in Cell II. Thus the hydrodynamic entrance length was 80 and 100 dia. for Cells I and II, respectively. A summary of pertinent dimensions of the cells is given in Table 1.

TABLE 1. DIMENSIONS OF THE EXPERIMENTAL CELLS (CM)

	Cell I	Cell II
Total Length	10.40	5.644
Entrance Length	7.80	3.735
Length After Electrodes	0.55	0.920
Width	1.00	1.00
	(1.5, 2.0)	
Height (Electrode Separation)	0.05080	0.01877
Cathode Dimensions		
Section I	0.39056	0.19680
Section II	0.40029	0.19745
Section III	0.79956	0.39795
Section IV	0.39828	0.19680
Hydraulic diameter	0.09530	0.03689
	(0.09692, 0.09904)	
Aspect ratio	20	53.2
	(30, 40)	
Pressure tap locations		
No. 1	0.70	1.1350
No. 2	2.6136	2.1669
No. 3	4.5240	2.6390
No. 4	6.4236	3.1398
No. 5	7.3824	3.6381
No. 6	8.7332	4.1432
No. 7	9.5346	4.5455
No. 8	10.1371	4.9310

Sectioned Electrodes

The four sections forming the cathode were cut of 99.9% pure nickel plate and machined to close specifications. The total length of the cathode was equivalent to 20 and 26 hydraulic dia. for Cells I and II, respectively. The length of the four sections in the axial (flow) direction was approximately 4, 4, 8, and 4 D_h, respectively, in Cell I; the length of the four sections of Cell II was 5.3, 5.3, 10.6, and 5.3 D_h. Short strips of 0.001 in. thick Mylar sheet were glued to one of their sides and then all the pieces were clamped together and cast in epoxy resin. After polishing, the surface of the sectioned electrode was flat and the insulating strips were barely noticeable. However, when the cells were sandblasted for the rough surface experiments, the insulating epoxy strips tended to erode more rapidly than the nickel segments, giving a more noticeable discontinuity. This imposes a limitation on the number of electrode segments employed. Under ideal conditions the velocity field over the electrode should be undisturbed, but such condition requires a completely smooth epoxy-nickel junction. In addition, there will be a discontinuity in the mass transfer boundary layer since the transfer process is interrupted at the insulator. Under actual conditions both the flow field and the mass transfer boundary layer are affected, and one will want to keep these disturbances to a minimum. In the turbulent regime even the smallest electrodes were too long to allow an exact determination of the mass transfer entrance length, and some uncertainty existed in the assignment of the local average mass transfer coefficient to a given point in the Sh versus x/D_h curve.

By a simple scheme, possible only when using electrochemical methods, the four cathode sections allowed the assignment of eight points in the curve of k (or Sh) vs. x/D_h: For Cell I, when the four sections were active (electrically connected to the power source) the points obtained corresponded to x/D_h values of approximately 2, 6, 12, and 18;* when section I was disconnected the points obtained corresponded to x/D_h values of 2, 8, and 14; with only sections III and IV active the x/D_h values were 4 and 10, while section IV alone gave again the average mass transfer coefficient for an x/D_h value of 2. For Cell II the halfway points corresponded to x/D_h values of 2.65, 5.3, 7.95, 10.6, 13.25, 15.90, 18.55, and 23.85.† By this scheme of successively disconnecting the upstream sections of the cathode the hydrodynamic entrance length was in effect increased by 4, 8, and 16 D_h in each instance.

Electrode Surface Preparation

Four types of roughness, in addition to hydraulically smooth walls, were used. Three of these roughnesses were of a random distribution, while the fourth was geometrically well defined.

One of the main difficulties in dealing with rough surfaces is their unambiguous characterization. In friction factor studies the surface roughness is typically characterized using the following procedure: friction factors are determined at very high Reynolds numbers (Nikuradse's "fully rough region") where the friction factor becomes independent of Re and depends solely on the value of the relative roughness. Then, by comparison with the f values

* For ease in understanding, here we refer to this average mass transfer coefficient as if it were assigned to a point halfway along the length of the electrode section. Correction for non-linear dependence of the mass transfer on distance from the leading edge was considered in presenting the results given in the text:

For laminar regime, the extension of the Graetz-Leveque to parallel plate channels (Newman, 1968) is

$$Sh = 1.2325\ (Re\ Sc\ D_h/x)^{1/3} \tag{5}$$

From this equation we can calculate the value of the distance x that would give a local mass transfer coefficient equal to the measured average mass transfer coefficient for a section of length L between $x = x_a$ and $x = x_b$:

$$x = \left[\frac{\frac{2}{3}L}{x_b^{1/3} - x_a^{1/3}}\right]^3 \tag{6}$$

According to the experimental result of van Shaw et al. (1963), mass transfer in the turbulent entrance regime is also characterized by a $-1/3$ power dependence on distance, with a fast approach to an asymptotic, fully developed, value of the mass transfer coefficient.

† The x/D_h values for Cell I, corrected for nonlinear dependence, were 1.197, 1.227, 1.220, 2.450, 5.846, 7.784, 10.237, 12,024, 14.404, and 18.484. For Cell II: 1.582, 1.587, 1.582, 3.200, 7.815, 10.114, 13.351, 15.685, 18.744, and 24.104.

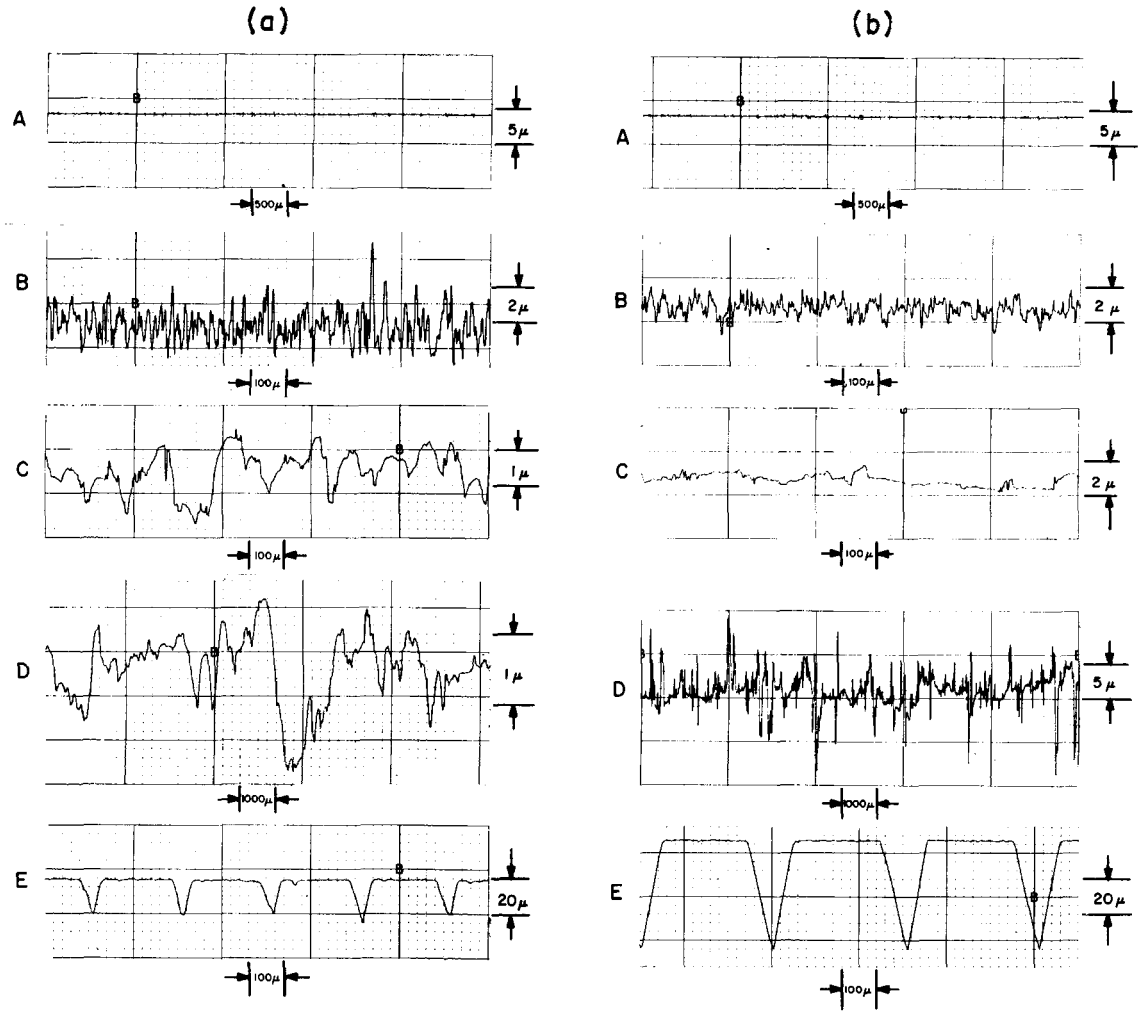

Figure 4. Profilometer traces (a) Cell II, (b) Cell I. (A) Hydraulically smooth; (B)–(E) roughness I to IV.

obtained by Nikuradse using sand-roughened pipes, an "equivalent sand roughness value" is assigned to the roughness in question. The argument for this procedure seems ponderous. In many cases the measured size of the roughness elements, even when sand grains are used, bears no relationship to the value obtained by the equivalent sand roughness determination. Also, the values of f obtained at intermediate Reynolds numbers may differ substantially for the same value of the equivalent sand roughness. Even if this method of roughness characterization were effective for momentum transfer studies, there is no valid reason to expect that it would work equally well for the case of mass transfer.

The rationale for including rough surfaces in the present study was the almost absolute absence of documented work on transport processes in rough channels where both the momentum and the mass transfer coefficient were measured in the same equipment. Since the transport processes depend on the type and degree of roughness, and there is no unequivocal method to specify them, no claim of generality is intended for the present results. The methods employed to obtain the different types roughness are given below. Samples of profilometer traces taken of the cells are shown in Figure 4. (Surfanalyzer Model 21-1330-20. Gould Inc., El Monte, CA.)

Hydraulically smooth channel: Because of the exceedingly small gap between electrodes and the resulting extreme thinness of the mass transfer boundary layer, it was found necessary to polish the cell to optical smoothness to obtain hydraulically smooth surfaces. The cell plates were milled and ground to make them flat prior to polishing. Polishing was done using a polishing wheel with velvet backing and diamond powder of 0.1 μm size. The cell plates were polished until flat to within two wavelengths (approx. 1.2 μm) over its entire surface.

Roughness I: This was obtained by sandblasting the surface with fine abrasive (27 μm mesh).

Roughness II: The surface of the cell was ground with a fine aluminum oxide wheel. The travel of the grinding wheel was always in the axial direction of the cell; hence, the roughness obtained was not strictly random. However, analysis of the roughness using a stylus profilometer showed the roughness to be independent of direction.

Roughness III: The surface of the cell was sandblasted using a coarse abrasive (mesh size 36).

Roughness IV: The surface was inscribed with V grooves running perpendicular to the flow direction. For Cell I these grooves were 0.0125 cm wide at the base, 0.005 cm deep at the apex of the triangle. The separation between neighboring grooves was 0.0250 cm (two times the width of the base). For Cell II the corresponding dimensions were 0.0075, 0.0025, and 0.0150 cm, respectively. These configurations were arbitrarily chosen. Even though this type of roughness is not normally present in rough electrodes, it was studied as an extreme case of the effect of roughness on the mass transfer coefficients.

DETERMINATION OF FRICTION FACTORS

Friction factor coefficients were determined from pressure drop measurements in the same flow channel used for the mass transfer experiments.

Pressure Taps

The channels were provided with eight pressure taps, five upstream of the mass transfer section, two in the mass transfer section,

and one downstream from it. Strain gauge pressure transducers were connected to each of the pressure taps. To affect the flow as little as possible by the presence of the tap openings, the diameter of the pressure tap holes had to be made as small as possible. The holes in the epoxy walls were drilled 0.0150 cm in diameter. In the electrodes proper, because of their harder material, holes 0.1 cm in diameter were drilled, and a short length of 0.01 cm ID tube that fitted snugly in the hole was inserted in them. This tube was manufactured from hypodermic stainless steel tube with a 0.02 cm OD on which nickel was electroplated until the necessary diameter was attained.

The friction coefficients were calculated from pressure drop measurements at the four points on the channel spanning the length of the mass transfer section. When the absolute values of the static pressure were plotted as a function of position, a line that becomes essentially straight for the four positions spanning the electrodes was obtained. This was taken as an indication that the entrance length provided was sufficient to allow for a fully developed flow at the mass transfer region.

The error introduced by the disturbance of the flow caused by the pressure tap holes is difficult to assess. It constituted the main source of inaccuracy of the pressure drop measurements. However, for smooth channels the opening of all the piezometric holes appeared to be of the same shape when inspected through an optical microscope, and it is reasonable to believe that any error introduced by the hole itself was substantially the same at each measuring station. Since we were interested in pressure differences only, it was assumed that these errors canceled out when the difference between two readings was taken. For channels with roughened walls it is difficult to ascertain that the roughness at the mouth of all the piezometric holes is the same. Since the turbulence created by the rough edge will be different from hole to hole, it is unwarranted to assume that the errors introduced by the presence of the hole cancel upon taking the difference between two pressure readings. Indeed, the results of pressure drop measurements conducted with these channels showed much more scatter.

Fluid Handling

Due to the very wide range of pumping pressures needed to run the experiments with the very small channel gaps used, two separate pumping systems were required (see Figure 5). The first pumping system consisted of a regenerative centrifugal turbine pump with a maximum head of 8.96×10^5 N/m^2 and a constant delivery of 2.2×10^{-4} m^3/s. For the largest Re studied when using the cell with $D_h = 0.038$ cm, the pressure drop through the flow channels demanded that a pumping system capable of delivering the working solution at pressures up to 20.7×10^6 N/m^2 be employed. The only mechanical pumps capable of delivering this head are those of the reciprocating type. However, these pumps give a pulsating flow, which made them undesirable for the present application. For this reason a pneumatic pump, capable of delivering a total volume of 9.5 L of solution at a maximum pressure of 24.8 $\times 10^6$ N/m^3 (245 atm) at the exit of the pump, was built for use in this range of pressure heads. The pneumatic pump consisted of a hydraulic accumulator used as a flow separator and a pressure regulator to fix the delivery pressure of the pump. The inside of the cast iron accumulator shell was nickel-plated to avoid contamination of the working electrolyte, while the bladder was of a butyl rubber composition that resists oxidation by the solution. The pneumatic pump was connected to the cell by means of 0.635 cm D stainless steel 304 tubing with a 0.0889 cm wall thickness. High pressure fittings and gate valves were used in this line. In operation the solution was pumped into the shell while the bladder was vented to the atmosphere. Once the shell was full, nitrogen gas at the pressure needed to obtain the required Reynolds number in the cell was fed into the bladder through a pressure regulator. When the valve controlling the flow of the solution was opened, the constant pressure that the nitrogen exerted on the butyl bladder forced the exit of the solution at a steady rate. In this manner, pulse-free flow at high pressure could be delivered to the cell. A disadvantage of this system is that the duration of the runs was limited by the capacity of the accumulator (9.5 L), coupled with the fact that once the pneumatic pump had been emptied it took approximately 10 min to bleed the nitrogen gas from the bladder and refill the shell with solution.

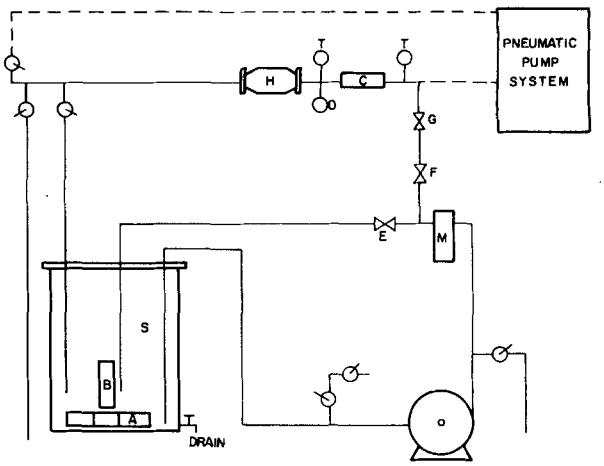

Figure 5. Schematic diagram of the test facility. A, Cooling coil; B, Heater; C, Experimental cell; D, Thermistor; E, F, and G, Needle valves; H, Magnetic flow meter; M, Cartridge filter; S, Polyethylene holding tank; T, Bimetallic thermometers.

When using the pneumatic pump the temperature control system could not be employed. These runs were performed at room temperature, quite constant at approximately 22°C. Also, since the pressure drop through a filtering medium would have been prohibitive for these runs, the solution was passed unfiltered through the cell for several runs and then filtered in the low pressure system before returning it to the pneumatic system.

RESULTS AND DISCUSSION

Friction Factor

The friction factors determined for the entire Reynolds number range are presented in Figure 6 in the form of f versus Re. For smooth walls, in both the laminar and the turbulent regimes, the data can be fitted to expressions of the type $f = B\,Re^n$. At low Reynolds numbers ($Re \leq 2{,}700$) the results indicate a linear relationship with a negative slope of -1. This is the type of dependence predicted by the Hagen-Poiseuille solution for smooth tubes: $f = 16/Re$. However, for these rectangular channels the coefficient B of that expression is larger. At high Reynolds number ($Re \geq 5{,}000$) the dependence of f on Re appears to be linear, following a line parallel to the well-known Blasius equation for smooth pipes. Again, the value of the coefficient is larger than for round ducts. The coefficient B in both the laminar and the turbulent regimes is larger than that found for round ducts, probably due to the effect of the channel corners, since additional momentum will be dissipated in the secondary flow currents.

In the intermediate Reynolds number range ($2{,}700 \leq Re \geq 5{,}000$) the value of the friction factor rises steeply following a trend that has been reported for smooth pipes and channels. The range over which this transition region extends is wider than that commonly reported for pipes, and the approach to a linear (fully turbulent) behavior is rather slow. Similar behavior has been reported by Patel and Head (1969) using a large aspect ratio (1:48) parallel plate channel.

At low Reynolds number (in the laminar regime) the value of the friction factor for the two smaller roughnesses coincides with that for the smooth channel. For the channel roughness III and IV, the friction factor also follows a fairly linear dependence on the Reynolds number, but the value of the slope is greater than -1, and the value of the coefficient is considerably larger than for the smooth channel.

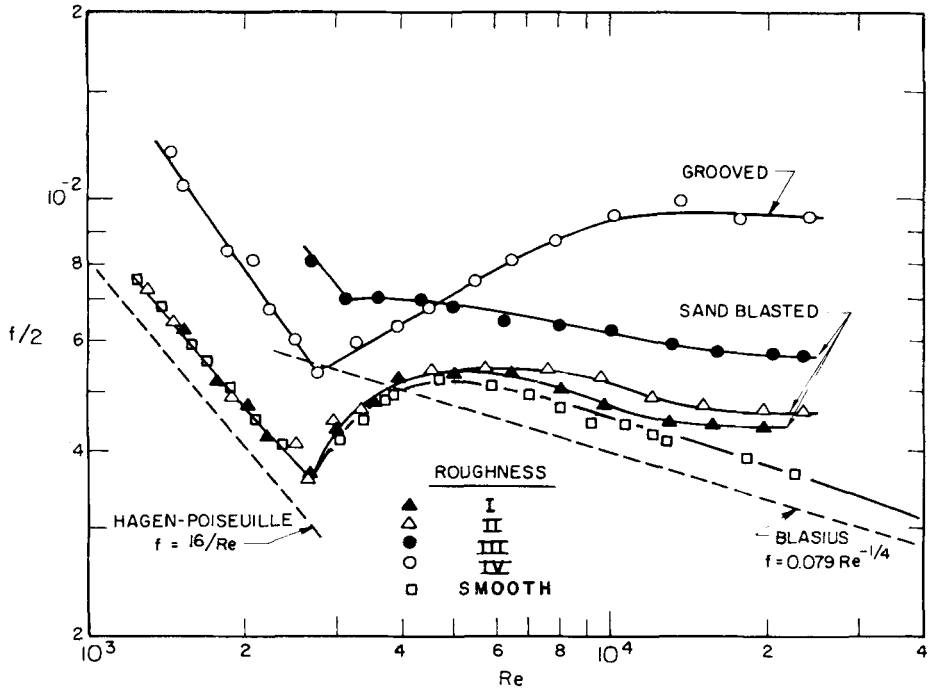

Figure 6. Experimental friction factors for Cell I.

For the case of the grooved surface it is possible to calculate in a fairly accurate manner the increased surface of the channel walls and hence to correct the value of f by the true drag force on the walls. Since the friction factor f is defined (Bird et al., 1960) by

$$F_k = A_{\text{wet}} K f$$

For flow without changes in potential energy through a channel with rectangular cross section wxg, the friction factor is given by

$$f = \Delta P(wxg)/(\tfrac{1}{2}\rho v^2)A_{\text{wet}}$$

From the measured value of the grooves, the increase in wetted area is approximately 13.7%. This correction would bring the value of the friction factor for rough surface IV closer to the value of f for the smooth walled channel, but there still would exist a disagreement. One explanation for this discrepancy is the fact that the value corrected for the increased surface still fails to include the form drag caused by the shape of the grooves.

The transition regime for roughness I and II extends through the same Reynolds number range as for the smooth channel, $2{,}400 \leq Re \geq 5{,}000$. As a matter of fact, the values of f for the smooth channel and roughness I and II are substantially indistinguishable in this range.

For roughness IV the transition regime extends through a wider Reynolds number range, $2{,}400 \leq Re \geq 10{,}000$, before f becomes independent of the Reynolds number.

Mass Transfer

Entrance Length. The average mass transfer coefficients for the individual sections were assigned to specific x/D_h values, assuming that the dependence on $x^{-1/3}$, Eq. 6, applies equally to mass transfer in smooth and rough channels. To date, no systematic studies have been conducted on the effect of wall roughness on the length of the mass transfer entrance length. Figure 7 presents the experimental results for Cell II, smooth. Sh_L was calculated using the value of k determined for the electrode farthest downstream (fourth section when all sections were polarized). It should be noted that all the data fall on smooth lines. As explained above, some of the intermediate points in the curve were obtained with longer values of the hydrodynamic entrance length (i.e., when the upstream electrodes were not polarized). If the hydrodynamic conditions at the electrode had been different for each value of the entrance length, the experimental points would oscillate around a smooth line. The fact that this was not the case gives further assurance that the flow was already fully developed at the location of the first electrode section.

From this figure it can also be seen that the data corresponding to $Re \leq 2{,}500$ all fall on the same line, as required by the unique solution for the purely laminar regime (Eq. 6). For larger Re (at $Re \geq 2{,}700$) the data fall on separate lines for each Re studied. The displacement of these curves from the position of the laminar results agrees with the trend predicted by Spalding's calculations (1961). At $Re = 18{,}000$ the entrance effect indicated by these data seems to extend to $x/D_h = 2.5$. This entrance length value is larger than those previously reported for tubes (van Shaw et al., 1963). Picket and Stanmore (1972) have also reported longer entrance lengths in rectangular channels. The limitation imposed by the relatively large size of the leading electrodes does not allow us to derive definitive conclusions regarding entrance length.

Due to the restrictions imposed by the size of the leading segments of the electrode, only qualitative conclusions could be drawn from the present experiments: rough surfaces lead to a departure from the laminar results at a lower Reynolds number, while at large

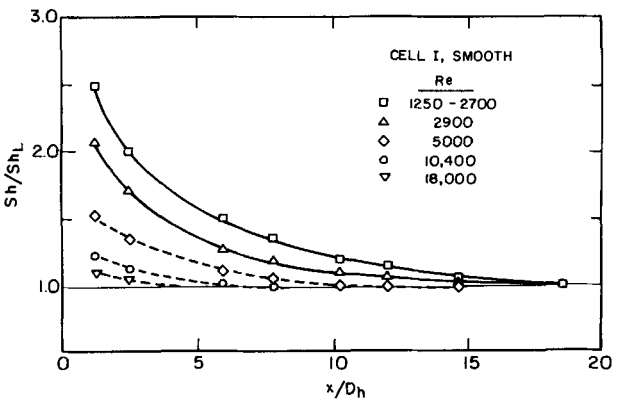

Figure 7. Dependence of the mass transfer coefficient on the distance from the mass transfer leading edge. Sh_L was calculated using the value of k for section IV when the four sections were polarized.

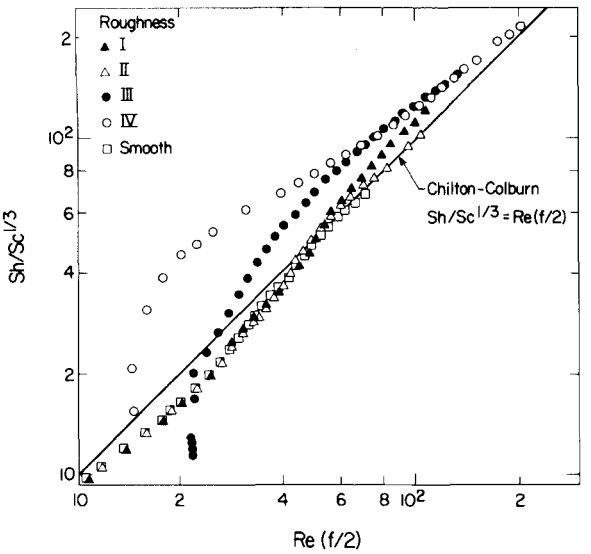

Figure 8. Comparison of the mass transfer coefficients and the friction factors experimentally determined for Cell I with the Chilton-Colburn correlation. *Sc* = 2,000 − 3,500.

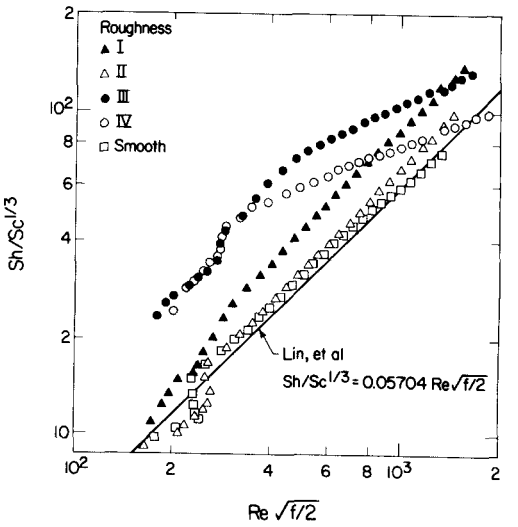

Figure 9. Comparison of the mass transfer coefficients and friction factors experimentally determined for Cell II with the correlation of Lin et al. *Sc* = 2,700 − 3,800.

values of the Re the entrance length becomes shorter than for smooth channels.

The first conclusion agrees with what would be expected from hydrodynamic considerations: the Reynolds number region of stability of laminar flow decreases with the turbulence induced by the roughness of the wall. The second conclusion can also be understood by similarity to the hydrodynamic case: One will expect that disturbances present at the point where the mass transfer boundary layer begins will act as "boundary-layer trippers" and will lead to its reaching the fully developed value faster, thereby shortening the entrance length.

Correlation of Mass and Momentum Transport. As stated in the introduction, one of the objectives of the present study was to test the applicability of turbulent mass transfer correlations available in the literature to the case of mass transfer in very thin channels. A review of correlations proposed in the past is beyond the scope of the present work. A thorough review of empirical and semiempirical mass transfer correlations was presented by Hubbard and Lightfoot (1966) and by Selman and Tobias (1978). Most of these correlations indicate that Sh depend on $Sc^{1/3}$ and on either $f/2$ or $(f/2)^{1/2}$. Accordingly, the values of Sh_{ave} determined for Cells I and II in the Reynolds number range $2{,}700 \leq Re \geq 22{,}000$ are presented in Figures 8 and 9 in the form $Sh_{ave}/Sc^{1/3}$ versus $Re(f/2)$ and $Sh_{ave}/Sc^{1/3}$ versus $Re(f/2)^{1/2}$, respectively.* In both cases the value of the friction factors used were those determined for the same experimental channel used to measure the mass transfer coefficients. For economy of space and for clarity only one type of plot is given for each cell; the general behavior of the data was the same for the two cells, except as indicated below.

For smooth wall channels at large values of the Reynolds number ($Re \geq 10{,}000$), the experimental data correlate well with both the Chilton-Colburn (1934) and the Lin et al. (1953) correlations. For most design purposes the simpler Chilton-Colburn equation could be used satisfactorily. This conclusion agrees with that reached by Hubbard and Lightfoot (1966).

For rough surfaces both the Chilton-Colburn and the Lin et al. equations fail to correlate the results within the range of Reynolds numbers studied. For Cell I, the trend of the points seems to indicate that at very large values of Re, the Chilton-Colburn equation may give an acceptable fit for surfaces with small roughness. For the case of Cell II, neither of the equations correlated the results, even for the smallest roughness used ($\epsilon/D_h = 0.005$, roughness II).

$j_D/f/2$ Ratio. Whether or not rough electrodes are advantageous for technological use depends on the specific application contemplated. A measure of the relative merit of mass transfer surfaces is the ratio $j_D/(f/2)$, this ratio being related to the mass transfer obtainable per unit of pumping power. Even though the Chilton-Colburn correlation ($j_D = f/2$) applies only at Reynolds numbers in the fully turbulent regime, and for the case of rough surfaces the friction factor includes the form drag, a departure from the value of 1 for this ratio can be used as an index of the effectiveness of a given roughness in increasing the transfer coefficient. It must be noted that the effect of the form drag will be to *increase* the value of $f/2$, and hence for rough surfaces one may be justified in expecting a *decrease* in the value of this ratio. In addition, j_D takes into account the transport process to the flat surfaces only, while $f/2$ reflects the effect of the corners.

Figure 10 presents the values of $j_D/(f/2)$ versus Re. From this figure it is seen that for electrodes with a small roughness value this ratio becomes larger than 1 only for $Re \geq 10^4$. On the other hand, for large roughness value the ratio reaches a maximum (greater than 1) in the transition region, and then rapidly drops toward a value of 1. Limitations in the experimental system did not allow operation at higher Re to ascertain if asymptotic behavior is

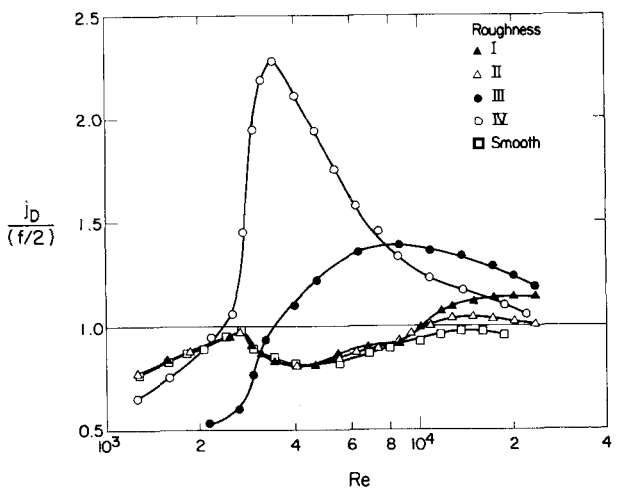

Figure 10. Ratio of the mass to the momentum transfer coefficient for Cell I. *Sc* = 3,000 − 3,500.

* The "kink" in the data for the cell with $D_h = 0.03689$ cm arises from anomalous f data obtained for this cell in the range $2{,}500 \leq Re \leq 4{,}000$. In this region of hydrodynamic transition the (relatively) large size of the pressure tap holes, plus any small differences in the shape of their opening, must have created disturbances that were substantially different from one tap to another. The value of ΔP, and hence f, evidenced this condition.

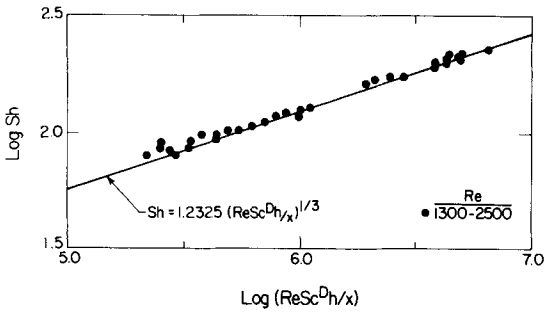

Figure 11. Comparison of the experimental *Sh* values obtained with Cell II with the Graetz-Leveque equation. The experimental values depart from the straight line at *Re* ≥ 2,650 for roughness I and at *Re* ≥ 2,800 for roughness II; for roughness III and IV the data deviated from the straight line at all *Re* studied.

reached for this ratio. (At the highest Reynolds number studied, the pressure drop for channel II, $D_h = 0.038$ cm, was already of the order of 20.6×10^6 N/m^2.)

Similar results for heat transfer have been reported by Dipprey and Sabersky (1963) for the ratio $j_h/(f/2)$. Their experiments were conducted at higher Reynolds numbers, $14{,}000 \leq Re \geq 120{,}000$, and for $1.2 \leq Pr \geq 5.94$. At the higher Pr values studied they found that the ratio $j_h/(f/2)$ reached a maximum at intermediate values of the Reynolds number, the position of this maximum depending on the value of the roughness. For the largest roughness employed ($\epsilon/D = 0.048$) the maximum apparently fell below the lowest Reynolds number at which they operated.

VALIDITY OF THE RESULTS

A test of the validity of the present results is the agreement of the mass transfer coefficients determined in the laminar regime with the extension of the Graetz-Leveque solution to the problem of flow in parallel plate channels (Eq. 5). Figure 11 shows that, for smooth electrodes, for $1{,}300 \leq Re \geq 2{,}750$ the spread of the data around the straight line with slope 1.2325 is only 1%. At $Re = 2{,}950$ the departure from the laminar behavior was noticeable, particularly at large values of x (low values of the abscissa). For each of the roughness values studied the departure of the data from the theoretical straight line with slope 1.2325 became evident at lower Reynolds numbers than for the smooth channel. The lowest value of *Re* at which the departure from the Graetz-Leveque solution was observed is indicated in the figure caption.

Effect of the Channel Corners

In rectangular cross-sectional flow channels the mass flux to the walls varies in the direction transverse to the flow due to secondary hydrodynamic currents at the corners of the channel. In previous work using the electrochemical technique two schemes have been used to obviate these variations: (a) the electrodes were made narrower than the channel (Hubbard and Lightfoot, 1966; Kitamoto and Takashima, 1970; Mizushina et al., 1971), or (b) "buffer" electrodes located along the longitudinal edges of the working electrode were used (Tobias and Hickman, 1965; Landau and Tobias, 1976) to absorb the effects of the secondary flows. The first scheme fails to account for the enhanced rates of mass and charge transfer to the edges of the electrode. The second scheme, although effective, requires a complicated electrode assembly and may give rise to undesirable effects if the electrode sections are not kept absolutely planar, a very difficult task when dealing with very small equivalent diameters.

In this work the effect of variations of the mass flux in the transverse direction on the calculated mass transfer coefficient was minimized through the use of very large aspect ratios. For laminar flow it is possible to calculate the effect that the side walls will have on the velocity profile (Happel and Brenner, 1965) and hence on the mass transfer coefficient. This calculation indicates that the effect will extend to a distance approximately equal to the interelectrode separation. This is consistent with the experimental results of Rousar et al. (1971), where the variation of the mass flux in the traverse direction was measured using one single aspect ratio. For the case of turbulent flow such calculation is not possible. However, determinations by Nikuradse of isovelocity lines (Schlichting, 1955) indicate that in turbulent flow the corner effect is also restricted to a distance smaller than the width of the narrower walls.

Comparison of the values of the mass transfer coefficient determined for the three different aspect ratios used with Cell I,

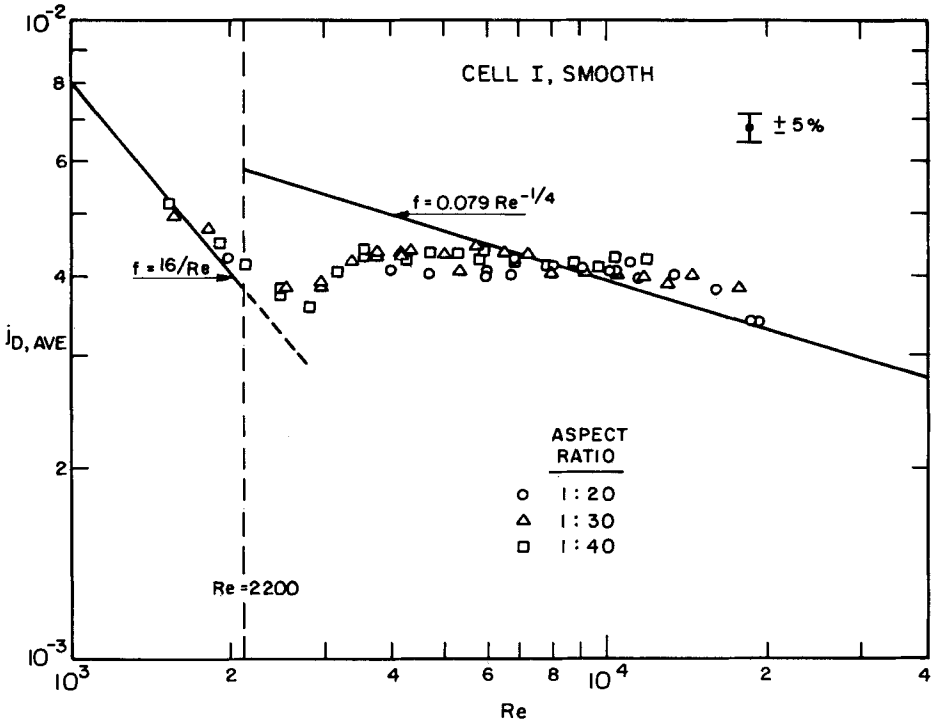

Figure 12. Effect of aspect ratio on the mass transfer coefficient, Cell I. *Sc* = 2,000 − 3,200.

smooth, are presented in Figure 12 in the form of j_D versus Re. From this figure it appears that for these large aspect ratios, the value of the mass transfer rate is independent of the aspect ratio employed. The values present a scatter of ±5%, but no trend with aspect ratio is discernible.

For rough channels the secondary flow currents formed at the corners will be affected by the degree and type of roughness of the wall; however, it is a nonuniformity of the roughness that would exert a decisive influence on the secondary currents. Since the value of the roughness was uniform across the width of the channel, and considering the results for smooth channels, it was deemed unnecessary to perform a complete set of experiments using different aspect ratios. Only two aspect ratios, 1:20 and 1:30, were used with Cell I, rough. The range of Reynolds numbers covered in this manner overlapped in the range $7{,}000 \leq Re \geq 10{,}000$. No effect of the aspect ratio was discernible.

ACKNOWLEDGMENT

This work was supported by the Director, Office of Energy Research, Office of Basic Energy Sciences, Materials Sciences Division of the U.S. Department of Energy, under Contract No. DE-AC03-76SF00098.

NOTATION

A_{wet} = wetted surface, cm^2
C = concentration, $gmol \cdot cm^{-3}$
D = diameter, cm
D = diffusivity, $cm^2 \cdot s^{-1}$
D_h = hydraulic diameter, D_h = 4 wetted area/perimeter, cm
F = Faraday's constant, 96,494 coulomb
F_K = total force exerted by fluid on duct surfaces, N
g = interelectrode gap, cm
h = heat transfer coefficient, $W \cdot cm^{-2} \cdot K^{-1}$
i = current density, $A \cdot cm^{-2}$
i_{lim} = limiting current density, $A \cdot cm^{-2}$
K = characteristic kinetic energy per unit volume, $N \cdot cm^{-2}$
k = mass transfer coefficient, $cm \cdot s^{-1}$
k_T = thermal conductivity, $W \cdot cm^{-1} \cdot K^{-1}$
N = molar flux, $gmol \cdot cm^{-2} \cdot s^{-1}$
ΔP = pressure drop, $N \cdot m^{-2}$
v = velocity, $cm \cdot s^{-1}$
w = width of the channel, cm
x = distance from the mass transfer leading edge, cm

Greek Letters

α = thermal diffusivity, $cm^2 \cdot s^{-1}$
ϵ = roughness, peak-to-peak, μm
ν = kinematic viscosity, $cm^2 \cdot s^{-1}$
ρ = density, $g \cdot cm^{-3}$

Subscripts

ave = average quantity
b = bulk quantity
o = Wall value

Dimensionless Numbers

f = friction factor
j_D = Chilton-Colburn factor for mass transfer, $j_D = Sh/(ReSc^{1/3})$
j_h = Chilton-Colburn factor for heat transfer, $j_h = Nu/(RePr^{1/3})$
Nu = Nusselt number, $Nu = hx/k_T$
n = Number of electrons exchanged in reaction,
Pr = Prandtl number, $Pr = \nu/\alpha$
Re = Reynolds number, $Re = Dv/\nu$
Sc = Schmidt number, $Sc = \nu/D$
Sh = Sherwood number, $Sh = kx/D$
t = Transference number for ionic species.

LITERATURE CITED

Acosta, R. E., "Transport Processes in High Rate Electrolysis," Ph.D. Thesis, Univ. of California, Berkeley (1974).

Bird, R. B., W. E. Stewart, and E. N. Lightfoot, *Transport Phenomena* Wiley, New York (1960).

Boeffard, A. J. L. P. M., "Ionic Mass Transport by Free Convection in a Redox System," M.S. Thesis, Univ. of California, Berkeley (1966).

Chilton, C. H., and A. P. Colburn, "Mass Transfer (Absorption) Coefficients. Prediction from Data on Heat Transfer and Fluid Friction," *Ind. Eng. Chem.*, **26,** 1183 (1934).

Dawson, D. A., and O. Trass, "Mass Transfer at Rough Surfaces," *J. Heat Mass Transfer*, **15,** 1317 (1972).

Dipprey, D. F., and R. H. Sabersky, "Heat and Momentum Transfer in Smooth and Rough Tubes at Various Prandtl Numbers," *Intern. J. Heat and Mass Transfer*, **6,** 329 (1963).

Eisenberg, M., C. W. Tobias, and C. R. Wilke, "Ionic Mass Transfer and Concentration Polarization at Rotating Electrodes," *J. Electrochem. Soc.*, **101** (1), 306 (1954).

Gordon, S. L., J. S. Newman, and C. W. Tobias, "The Role of Ionic Migration in Electrolytic Mass Transfer Diffusivities of Ferricyanide and Ferrocyanide in KOH and NaOH Solutions," *Ber. Bunsen. Phys. Chem.*, **70** (4), 414 (1966).

Happel, J., and H. Brenner, *Low Reynolds Number Hydrodynamics*, Prentice-Hall, Englewood Cliffs, N.J. (1965), p. 38.

Hubbard, D. W., and E. N. Lightfoot, "Correlation of Heat and Mass Transfer Data for High Schmidt and Reynolds Numbers" *Ind. Eng. Chem. Fundamentals*, **5** (3), 370 (1966).

Kitamoto, A., and Y. Takashima, "Ionic Mass Transfer in Turbulent Flow by Electrodialysis with Ion Exchange Membranes," *J. Chem. Eng. Japan*, **3** (2), 182 (1970).

Landau, U. "Distribution of Mass Transfer Rates Along Parallel Plane Electrodes in Forced Convection," Ph.D. Thesis, Univ. of California, Berkeley (1976).

Lin, C. S., R. W. Moulton, and G. L. Putnam, "Mass Transfer Between Solid Wall and Fluid Streams," *Ind. Eng. Chem.*, **45,** 636 (1953).

Mizushina, T., F. Ogino, Y. Oka, and H. Fukuda, "Turbulent Heat and Mass Transfer Between Wall and Fluid Streams of Large Pr and Sc Numbers," *Intern. J. Heat and Mass Transfer*, **14,** 1705 (1971).

Newman, J. S., "Engineering Design of Electrochemical Systems," *Ind. Eng. Chem.*, **60** (4), 12 (1968).

Patel, V. S., and M. R. Head, "Some Observations on Skin Friction and Velocity Profiles in Fully Developed Pipe and Channel Flows," *J. Fluid Mech.*, **38,** Part 1, 181 (1969).

Picket, D. J., and B. R. Stanmore, "Ionic Mass Transfer in Parallel Plate Electrochemical Cells," *J. Appl. Electrochem.*, **2,** 151 (1972).

Rousar, I., J. Hostomsky, and V. Cezner, "Limiting Local Current Densities for Electrodes Located on the Walls of a Rectangular Channel with Laminar Flow. Asymptotic Solution and Experimental Verification," *J. Electrochem. Soc.*, **118**(6), 881 (1971).

Schlichting, H. *Boundary Layer Theory*, McGraw-Hill, New York (1955).

Selman, J. R., and C. W. Tobias, "Mass Transfer Measurements by the Limiting Current Technique," *Adv. in Chem. Eng.*, T. B. Drew et al., eds, **10,** 211 (1978).

Son, J. S., and T. J. Hanratty, "Limiting Relation for the Eddy Diffusivity Close to a Wall," *AIChE J.*, **13,** 689 (1967).

Spalding, D. B., "A Single Formula for the 'Law of the Wall'," *J. Appl. Mech.*, **28,** 455 (1961).

Tobias, C. W., and R. G. Hickman, "Ionic Mass Transport by Combined Free and Forced Convection," *Z. Phys. Chemie*, **229,** 145 (1965).

Tuckerman, D. B., and R. F. W. Pease, "High-Performance Heat Sinking for VLSI," *IEEE Electron Device Letters*, **2,** 126 (1981).

van Shaw, P., L. P. Reiss, and T. J. Hanratty, "Rates of Turbulent Transfer to a Pipe Wall in the Mass Transfer Entry Region," *AIChE J.*, **9,** 362 (1963).

Manuscript received Apr. 29, 1983; revision received Jan. 17, 1984, and accepted Jan. 28.